Modelling approach to the assessment of biogenic fluxes at a selected Ross Sea site, Antarctica

Vichi M.[1*], Coluccelli A.[1**], Ravaioli M.[2], Giglio F.[2], Langone L.[2], Azzaro M.[3], Azzaro F.[3], La Ferla R.[3], Catalano G.[4], Cozzi S.[4]

1 INGV, Sezione di Bologna, Via Creti 12, 40128 Bologna, ITALY

2 CNR-ISMAR Sezione di Bologna. Via Gobetti 101, 40129 Bologna, ITALY,

3 CNR-IAMC Sezione di Messina. Spianata S. Ranieri 86, 82122 Messina, ITALY.

4 CNR-ISMAR Sezione di Trieste. V.le Gessi 2, 34123 Trieste, ITALY.

Abstract

Several biogeochemical data have been collected in the last 10 years of Italian activity in Antarctica (ABIOCLEAR, ROSSMIZE, BIOSESO-I/II). A comprehensive 1-D biogeochemical model was implemented as a tool to link observations with processes and to investigate the mechanisms that regulate the flux of biogenic material through the water column. The model is ideally located at station B (175^{o}E - 74^{o}S) and was set up to reproduce the seasonal cycle of phytoplankton and organic matter fluxes as forced by the dominant water column physics over the period 1990-2001. Austral spring-summer bloom conditions are assessed by comparing simulated nutrient drawdown, primary production rates, bacterial respiration and biomass with the available observations. The simulated biogenic fluxes of carbon, nitrogen and silica have been compared with the fluxes derived from sediment traps data. The model reproduces quite well the magnitude of the biogenic fluxes, expecially those observed in the bottom sediment trap, but the peaks are delayed in time. Sensitivity experiments have shown that the characterization of detritus, the choice of the

sinking velocity and the degradation rates are crucial for the timing and magnitude of the vertical fluxes. An increase of velocity leads to a shift towards observation but also to an overestimation of the deposition flux which can be counteracted by higher bacterial remineralization rates. Model results suggest that observed fluxes could be explained by the size-distribution and quality of the locally-produced biogenic material. It is hypothesized that the bottom sediment trap collects material originated from rapid sinking of particles and also from previous years production periods, likely modulated by advective and aggregation mechanisms which are still not resolved by the model.

Key words: biogeochemical model, BFM, ERSEM, carbon flux, sediment trap, Ross Sea

---

1 Introduction

More than 10 years of physical and biogeochemical measurements have been collected in the framework of the Italian Programme for Antarctic Research (PNRA, Progetto Nazionale di Ricerca in Antartide). These data represent a valuable set of information on the dynamical variability of polar ecosystems and can be profitably used to constrain biogeochemical models of the global ocean carbon cycle in the Southern Ocean. On the other hand, models can also be used to support the interpretation of observations, as tools to link data with processes and to investigate the complex mechanisms that regulate the flux of biogenic material through the water column.

We have a fragmented picture of the plankton seasonal cycle in the Ross Sea, mostly derived from composites of diverse biogeochemical data collected in different years (Smith et al., 1996, 2000; Lipizer et al., 2000; Smith and Asper, 2001; Azzaro et al., 2006). Little synoptic observations are available, and the longer seasonal timeseries on biogenic components are obtained from sediment trap measurements

(Collier et al., 2000; Langone et al., 2000). Phytoplankton growth in the Ross Sea is initiated in early spring, much earlier than in other regions of the Antarctic, likely because of favourable stratification conditions induced by ice melting (Smith and Asper, 2001). The patchy structure of this process is therefore responsible of the large spatial variability of growth conditions. After the onset of stratification, the spring-summer period is characterized by spatially-extended blooms dominated by diatoms in the north-eastern open water part and by the colonial prymnesiophyte *Phaeocystis Antarctica* in seasonal ice zones and coastal waters (DiTullio et al., 2000; DiTullio and Smith, 1996).

The vertical fluxes of biogenic material are characterized by the occurrence of rapid sinking events (DiTullio et al., 2000; Asper and Smith, 2003; Langone et al., 2003), time-stretched small deposition rates that lag the production peak of some months (Gardner et al., 2000; Collier et al., 2000) or by a combination of both phenomena (Langone et al., 2000). It is thus difficult to assess the overall impact on the CO_2 fluxes with the atmosphere and the definitive sequestration rates of organic carbon in the deep sediments. Organic fluxes through the water column are apparently a small fraction (5-8%) of the surface production (Langone et al., 2003; Smith and Dunbar, 1998) although moorings located in regions such as the Joides basin indicate that deeper deposition rates are more than double the flux collected in shallow trap sediments above (Collier et al., 2000; Langone et al., 2000). This suggests that processes other than surface export modify the characteristics of the sinking material, the more likely being horizontal advective transport and aggregation mechanisms.

To partly bridge the gaps among these contrasting information, we have implemented a coupled physical-biogeochemical model at station B (175^oE - 74^oS, central Joides basin, Fig. 1) of the PNRA Italian programme, with the aim to reproduce

the locally-produced organic matter vertical fluxes as forced by the dominant water column physics. The ultimate scope of the simulation is thus not to fit the sparse observations, but rather to provide the dynamical framework for hypotheses testing, verifying the model prediction against the available standing stock and rate measurements collected during the Italian and international joint projects (ABIOCLEAR, ROSSMIZE and BIOSESO-I/II). Particularly, this work will focus on the assessment of the vertical fluxes of organic particles and the comparison with data collected in sediment traps. Station B was chosen for several reasons: the more simple physical conditions due to the absence of polynia, a diatom-dominated bloom instead of Phaeocystys (which reduces the complexity of the phytoplankton parameterization) and also because many open questions still remain on the vertical dynamics inferred from sediment traps with respect to other more typical mooring sites (station A', 76.8^{o}S 169^{o}E, Langone et al., 2003)

The next section gives some details on the model features and the interannual forcing functions used to drive the one-dimensional simulation. Section 3 presents model results organized following these major guidelines:

- quantification of the organic matter production in the euphotic layer and comparison with available observations;
- quantification of heterotrophic consumption processes in the mesopelagic layer;
- estimation of model-derived sinking rates at given depths below the aphotic zone;
- comparison with sediment traps data.

Section 3.6 gives an overview of the model sensitivity to the key parameters affecting the vertical fluxes such as sinking velocity and bacterial remineralization rates. The outcomes of the experiments are discussed in Sec. 4 and, finally, Sec. 5 offers some conclusive remarks .

2 The simulation tool

The modelling framework is derived from the system set up by Vichi et al. (2004) to study the open Baltic biogeochemistry. The physical model is a vertical one-dimensional version of the Princeton Ocean Model (Blumberg and Mellor, 1987, POM), where the dynamical core is the turbulence closure scheme proposed by Mellor and Yamada (1982). The total depth of the water column is 588 m and the discrete vertical grid is composed of 30 levels, 5 in the first 20 m with a depth increasing from 1 to 10 m, and the reminders with a constant depth of 22 m.

The biogeochemical model is a further evolution and complete recoding of the European Regional Seas Ecosystem Model (Baretta et al., 1995; Baretta-Bekker et al., 1997, ERSEM). The Biogeochemical Flux Model (BFM) was developed in the framework of the European project MFSTEP (Mediterranean Forecasting System Towards Environmental Predictions, `http://www.bo.ingv.it/mfstep`) as a generalized modelling tool to be coupled to several kind of hydrodynamical models. This model was also applied to the world ocean ecosystem with a global configuration named PELAGOS (PELAgic biogeochemistry for Global Ocean Simulations **??**) which shows particular skills in the Southern Ocean. A formal background theory of the model applied to the global ocean is found in **?**, while an extended description of model equations and parameters is available on the model web site [1] . The model version used in this application is the standard BFM configuration with the addition of the iron dynamics used in PELAGOS and the further implementation of two forms of sinking organic detritus.

The biogeochemistry model is essentially a biomass-based set of differential equations that allows the description of processes involving the lower trophic levels and

[1] http://www.bo.ingv.it/bfm

major inorganic and organic components of the marine ecosystem. The model is based on the definition of Chemical Functional Families (CFF, **?**) which are further subdivided into living, non-living and inorganic components. Living CFFs are the basis of Living Functional Groups (LFG), the biomass-based functional prototype of the real organisms. LFGs are grouping of organisms according to their functional behavior in the ecosystem and to to phylogenetic considerations. Both CFFs and LFGs represent the concentrations of measurable properties of marine biogeochemistry such as the carbon content in marine diatoms or the nitrogen contained in dissolved organic matter (Fig. 2). All the model state variables are expressed in terms of several basic components (both elements as C, N, P, Si, O, Fe or biochemical molecules as chl).

As depicted in Fig. 2, the model resolves 4 different LFGs for phytoplankton (diatoms, autotrophic nanoflagellates, picophytoplankton and large phytoplankton), 4 for zooplankton (carnivorous and omnivorous mesozooplankton, microzooplankton and heterotrophic nanoflagellates), 1 LFG for bacteria, 8 inorganic CFFs for nutrients and gases (phosphate, nitrate, ammonium, silicate, dissolved iron, reduction equivalents, oxygen, carbon dioxide) and 11 organic non-living CFFs for dissolved and particulate detritus. The state variable nitrate is assumed here to be the sum of both nitrate and nitrite. With this kind of approach, all the nutrient:carbon ratios in chemical organic and living functional groups, as well as chl:C ratios in phytoplankton, are allowed to vary within their given ranges and each component has a distinct biological and physical time rate of change. This kind of parameterization mimics the adaptation of organisms to the prevailing nutrients and light conditions, and allow the recycling of organic matter to be functionally determined by the actual nutrient content.

2.1 Forcing functions and initial conditions

The model is forced with daily surface fluxes from the ERA40 data set over the period 1990-2001 (Uppala, 2001; Simmons, 2001) in a $1^o \times 1^o$ degrees region around station B. Daily sea surface temperature (SST) data from the Reynolds data set (Reynolds, 1988) are also used to restore the model SST with a relaxation term of 1 day. This strong nudging rate is needed to impose a consistent evolution of the sea ice cover. Wind stress and downward radiation flux are set to zero when the computed SST is below the freezing point, while the relaxation term is continuosly given to allow the surface to shift from packed-ice to ice-free conditions as typical of this marginal ice zone.

The model is initialized on June, 1st 1990 with average temperature, salinity and macronutrient profiles of the whole Ross Sea from the World Ocean Atlas (Conkright et al., 2002). Initial iron concentration is set to 0.25 μmol m^{-3} as the average value measured by Sosik and Olson (2002) in the Ross Sea. Biogeochemical LFGs and CFFs are initialized with homogeneous low values mimicking the quiescent winter period. The model is robust to the choice of winter initial conditions in the sense that the difference in the solution trajectories after one year of simulation is limited to less than 5%.

Nutrients are dynamically relaxed to the initial profiles when the water column is under packed-ice conditions, parameterizing the replenishment of nutrients caused by non-resolved vertical mixing and three-dimensional advection processes.

2.2 Model adaptation

Organic particle dynamics is complex and as a first approximation linked to the constituents and dimensions of particles. The standard BFM configuration assumes that organic detritus can be described by one single class of medium-degradable organic matter with a sinking speed of 1.5 m d^{-1}. This is a rough approximation because there is no distinction between denser, fast-sinking detrital material such as faecal pellets and other particulate excretion from smaller heterotrophs, lysis or sloppy feeding products. To differentiate between these groups an additional variable was introduced in the model representing the detritus produced by mesozooplankton (including biogenic silica frustiles of grazed diatoms). This CFF ($R_i^{(5)}$ in Fig. 2) has 5 components (C, N, P, Si and Fe) and is assumed to sink with a nominal velocity of 100 m d^{-1}. Measurements in the Ross Sea have in fact reported sinking speed of organic aggregates of more than 250 m d^{-1}(Asper and Smith, 2003). Sensitivity experiments have been carried out and presented in Sec. 3.6 to analyze the impact of different choices of the organic detritus parameterization on the results.

3 Simulation results

3.1 Water column physics

Fig. 3 shows the timeseries of the simulated SST, which is mostly controlled by the Reynolds data due to the imposed relaxation constraint. There is a clear interannual variability in the data which is also visible in the atmospheric forcing functions. The maxima in 1992 and 1997 are likely to be related to the large scale variability induced by ENSO, for which correlations have been reported with sea-ice retreat in the Ross Sea (Ledley and Huang, 1997; Kwok and Comiso, 2002).

The variability in the deeper part of the water column is much reduced and the surface signal does not propagate below the first 100 m. Langone et al. (2000) have reported a much larger seasonal variability of temperature at 200 m in the station B mooring. Nevertheless, the long-term vertical structure computed by the model is comparable with the average of the data collected during the deployment and monitoring of the mooring in the 1994-1998 summer campaigns (Fig. 4, Russo et al., 1997). The peculiar dicothermal layer is rather well reproduced by the model. This cold water structure, constrained between the surface warm waters above and the warmer waters below, is found in the surface layers of high latitude oceans generally between 50 and 150 m depth. Despite a slight discrepancy of 1 model level (22 m) in the location of the minimum, the vertical structure is in good agreement with the available observations, especially in the extent of the surface mixed layer.

3.2 Water column biogeochemistry

The simulated nutrient timeseries at the surface are shown in Fig. 5 and compared with the observations from the ROSSMIZE and BIOSESO I campaigns in the station B area (Catalano et al., unpubl.). Data were collected in December 1994 before the starting of the bloom and during "nutrient-depleted" conditions in January 1995 and 1996. Due to the low time resolution, it is not possible to infer a clear signal of the exact timing of the bloom. If we assume an ergodic hypothesis in the data disribution, we can say that the model broadly capture the range of the nutrient drawdown. The most remarkable feature is the discrepancy in the silicate uptake, which is underestimated even if the simulated bloom is composed of about 60% diatoms and 40% nanoflagellates (not shown). These results are obtained by taking into account an increased Si:C reference ratio of 3 times the standard BFM value due to the effects of Fe limitation (Takeda, 1998; Lancelot et al., 2000), but still the

model is not capable to reproduce the observed decrease in silicate concentration.

Autotrophic biomass (as chlorophyll concentration) and gross primary production (GPP) in the euphotic zone over the simulation period are shown in Fig. 6. Station B has a much lower biomass and production rates with respect to the stations in the polynia open waters (Smith et al., 1996, 2000), although the marginal ice zone can reach substantially high production rates and concentrations during the Austral spring (Saggiomo et al., 1998). The model simulates a bulk biomass and GPP rates which are comparable with the available observations (Saggiomo et al., 1998, 2002; Vaillancourt et al., 2003). GPP is highly correlated with SST in the model ($r = 0.91$, $p < 0.01$) and the periods with lower temperatures correspond to the minima of gross production. The chl content is instead less sensitive to temperature values but still significantly correlated ($r = 0.68$, $p < 0.01$). The production peaks are earlier by about one month with respect to the biomass maxima as also observed in the polinya region (Smith et al., 2000). However, in contrast with the latter observations, the model indicates that the maximum of production is in late January-February, and not in December. The nutrient observations are in partial agreement with the model showing a nutrient minima in early February, but the low sampling frequency is not sufficient to corroborate the model results.

Vaillancourt et al. (2003) also provide some information on the light regime at station B (station "Sei" of the US-JGOFS programme) during the Austral summer of 1997. The euphotic zone depth was around 40 m and the light diffuse attenuation coefficient was 0.122 m^{-1}. Simulated Chl concentration during this period is lower, and also the chl-specific primary production is about half the reported value of 11 mg C (mg chl)$^{-1}$ d^{-1}. The modeled euphotic zone depth is therefore slightly higher than observed. Furthermore, this diffuse attenuation coefficient is only obtained in the simulation by assuming a background attenuation of 0.08 m^{-1} (about twice

the optical attenuation of pure seawater) and a spectrally-integrated chl-specific light absorption of 0.03 (mg chl)$^{-1}$ m^2. The reported values in the polynia region dominated by *Phaeocystis Antarctica* are around 0.01 (mg chl)$^{-1}$ m^2 at the 676 nm red peak (Vaillancourt et al., 2003), but we may assume that a diatom-dominated population can have a larger value due to pigment packaging.

3.3 Phytoplankton light acclimation and growth rates

Several authors have suggested that the Ross Sea phytoplankton is adapted to low irradiance and therefore it should not be considered light-limited (Saggiomo et al., 2002; Smith et al., 1996). It is thus important to verify that the model is capable to reproduce these conditions and particularly the low specific growth rates typical of this region (Smith et al., 1999). Fig. 7a shows the simulated seasonal evolution in 1996-1998 of the realized chl:C ratio in surface diatoms, superimposed to the optimal value that is used in the model to drive chl synthesis according to the Geider et al. (1996) parameterization. Low chl:C ratios are characteristic of the Ross Sea (Smith et al., 1996). In stations dominated by diatoms, the chl:C ratio was as low as 0.005 (DiTullio and Smith, 1996), which is a value also predicted by the model as the minimum allowed. It is interesting to note that the realized ratio varies less than the potential value because of the water column mixing that homogenizes population adapted to different depths and light conditions.

Fig. 7b shows the simulated diatom specific growth rate in the surface layer computed with two different methods: i) estimated from the algebraic sum of the realized specific physiological rates of gross production, rest and activity respiration and activity excretion (cfr. Fig. 2); ii) computed from the surface carbon biomass stored every day of simulation and according to the formula used in field estimates

(Smith et al., 1999, 2000),

$$\mu = \frac{1}{\Delta t} \ln \left(\frac{C + \Delta C}{C} \right)$$

where C is the biomass concentration and ΔC the biomass change in the sampling interval $\Delta t = 1\,d$. The estimated growth rates of diatoms with the latter method are extremely low during the summer season, generally around 0.1 d^{-1} (Smith et al., 1999, 2000). The model agrees well with these estimates, implying that the net carbon production rates are reasonably simulated. However, these values are achieved only by applying a 0.5 coefficient to the non dimensional temperature regulating factor of phytoplankton growth based on the Q10 function (**?**). Indeed, Smith et al. (1999) suggest that the maximum growth rates predicted by the Eppley model (rather similar to the Q10 equation used in this model) overestimates growth at temperature lower than 2^oC. Goldman and Carpenter (1974) values are in fact about a half of the ones generated with the Eppley curve. Model results also suggest that the choice of the method can lead to different values. The thick line in fact represents the growth induced by local light and nutrient conditions, as the one obtained from controlled on-deck incubations. It is also visible a decrease during the maximum productive periods due to self-shading effects. The thin line is instead the realized change of mass due to a combination of physiological processes, vertical mixing and grazing rates. This is more similar to what can be measured in-situ, and is less representative of the physiological state of phytoplankton.

3.4 Microbial respiration

There are little information on the oxidation of organic matter in the mesopelagic layer of the Ross Sea. A recent work by Azzaro et al. (2006) provides the first estimates of microbial respiration in the aphotic zone, pointing out that about 63%

of the organic carbon remineralized by respiration derived from the detrital pool. Indeed, the model predict a very low concentration of DOC due to the excess of macronutrient availability, which reduces the release of polysaccharides from nutrient-limited autotrophic cells.

We have used the estimates of Azzaro et al. (2006) to assess the capability of the model to reproduce the remineralization of organic matter in the mesopelagic layer. Figure 8 shows the simulated vertical distribution of bacterial biomass and respiration rate during the period of the 2001 BIOSESO II campaign. The depth-integrated value of microbial biomass at site B in the mesopelagic layer (100-600 m), estimated from the measured ATP, varied from 480 to 840 mg C m^{-2}, and the depth-integrated respiration-derived carbon flux, calculated from direct ETS measurements, was 17.3 mg C m^{-2} d^{-1}. Both in the pre-bloom and bloom conditions (mid January and late February, respectively), the model shows a surface maximum of microbial respiration, with small subsurface maxima at 500 m. Bacterial biomass shows the same pattern in January, with a relative maximum in the deeper part. In February, the larger amount of freshly produced particles allows bacteria to homogeneously distribute over the whole water column, but still showing the maximum at 500 m. Bacterial respiration eventually increases during late summer-autumn, following the bulk of organic matter produced in the euphotic zone that reaches this depth in April-May (cfr. sections below). Integrated values are in reasonable agreement with the available observations, implying that the bulk of the remineralization process is rather well captured by the model.

3.5 Simulated sediment trap fluxes

Fluxes at the depth of the real sediment traps locations were computed as the product of the prognostic detritus concentrations at the selected depth with the respective sinking velocity. Figure 9 shows the comparison of model results with the fluxes estimated in the bottom-tethered trap at about 550 m (Langone et al., 2000) for organic C, N and biogenic silica (BSi). The peaks of the simulated fluxes are delayed by about 2 months with respect to the observations. Simulated maxima are quasi-simultaneous with the surface peaks in biomass, as indicated by the triangles in the upper axes of each subplot. This implies that the occurrence of the peak in the simulated trap is linked to the timing of the bloom, which is in turn linearly correlated with the SST.

On the other hand, the amplitude of the simulated C flux is in good agreement with the observations, and also the increase between 1995 and 1996, which is explained by the model as a response to the changes in SST and surface primary production. The fluxes of organic N closely follow the time distribution both in the data and in the model, but are overestimated by a factor 2-3. BSi is instead underestimated with respect to the trap data, which is likely to be related to the low consumption of dissolved silicate in the surface layers (Fig. 5).

The simulated deposition flux can be separated in the components due to the fast-sinking detritus produced by mesozooplankton and to the slow-sinking detritus for the surface and bottom traps (Fig. 10, for the C component only). In contrast with the observations (Langone et al., 2000), the peak in the top trap (Fig. 10a) is higher than the bottom trap during the productive phase and is mostly composed of large fast-sinking particles. The maximum of slow detritus is simulated in middle winter, with a lag of about 3 months with respect to the surface production peak as also

found in other sediment trap data (Collier et al., 2000). The bottom trap (Fig. 10b) is instead characterized by a summer peak mostly composed of slow detritus produced in the year before. This is followed by the peak of freshly-produced organic matter that sinks down with a velocity of 100 m d^{-1} and reaches the bottom trap almost at the same time of the trap above. It is interesting to note that there are periods such as late-spring and early-summer in which the bottom trap simulated flux is larger than the one above as also found in the observations (Langone et al., 2000).

3.6 Sensitivity analysis

The results shown in the previous sections have been obtained after a set of sensitivity analysis on the types of simulated detritus and their respective sinking and degradation rates. Table 1 reports the experiments that have been performed and the effects on the simulated vertical carbon fluxes at the sediment traps are depicted in Fig. 11. Experiment D0 is the standard BFM setup with one single type of detritus $R^{(6)}$ (Fig. 2); experiment D5 is the reference simulation run that have been previously described.

The difference between D0 and D1 shows the effect of the addition of another detrital component, $R^{(5)}$. With one slow-sinking detritus, the flux at the top trap is composed of one single peak that lags by 4 months the maximum of surface biomass and by 5 months the maximum of production. In D1, the addition of a relatively fast-sinking (10 m d^{-1}) component produced by the diatom grazers shifts the surface peak towards the bloom period and reduces the winter maximum. The same also occurs to a lesser extent in the bottom trap. The choice of the degradation rate of $R^{(5)}$ detritus determines the amplitude of the summer peak. In run D2 the

rate is decreased of 1 order of magnitude, while in D3 is set to 0.5 d^{-1}, equivalent to the availability of freshly-produced DOM. It is important to remember that these coefficients represent the availability of substrate to bacteria. Part of the substrate available to bacteria is converted to CO_2 and biomass in the model, but a fraction of it is also moved to the slow-sinking and less degradable compartment simulating a decrease of the organic matter quality. When the degradation rate is slow as in D2, more $R^{(5)}$ reaches both traps; when, conversely, the rate is higher as in D3 and the sinking rate is still 10 m d^{-1}, almost no fast-sinking detritus is found.

Setting the sinking rate to 100 m d^{-1}(run D4 and D5) shifts the deposition maxima towards the timing of the surface bloom but also lead to an overestimation of the deposition rates at both traps with respect to the observations. Only by assuming a large availability of $R^{(5)}$ as in D5, the reference simulation, it is possible to obtain simulated fluxes which are comparable with the data. Noteworthily, and despite the large overestimation, run D4 shows a larger flux in the bottom trap with respect to the one above, as also observed in data from station B moorings (Langone et al., 2000; Collier et al., 2000).

4 Discussion

The material collected in sediment traps is the result of a dynamical balance between the net export rate due to euphotic production, and the degradation and sinking rates, which are mostly determined by the size and quality of the particles. All these processes occur simultaneously in the upper ocean, and thus the estimation of vertical fluxes by means of surface sediment traps is affected by several biases (Buesseler, 1991; Smith and Dunbar, 1998; Buesseler, 1998). The use of numerical models is a possible mehodology to support the assessment of the organic

matter fate in the deep ocean, particularly in key regions like the Southern Ocean where the collection of long term timeseries is limited. Within the limits of the one-dimensional assumption, the production of organic matter in the upper ocean was simulated as a function of physical conditions, light and nutrient availability, and the prognostic vertical flux of organic material at selected depths was used to compare with deep-ocean sediment traps. Comprehensive biogeochemical models like the BFM can provide some of the dynamical linkages between observations derived from multidisciplinary campaigns. However, biogeochemical models need to be applied with due attention, because of the many assumptions in the parameterization of physiological and ecological processes (**?**).

The BFM has many parameters which can be adjusted to reproduce the observed biogeochemical system behaviour. Data constraints in the Ross Sea region are limited and therefore a model tuning is not possible. Since the model was mostly developed for temperate regions, we have performed a set of classical sensitivity analysis to identify the parameters which affect the biogeochemical processes under high latitude environmental conditions. The key parameters affecting the succession of phytoplankton groups are the basal respiration rates which determine the survival standing stock during wintertime. For this purpose, the standard BFM values have been halved for all the functional groups. This implies the need to refine the parameterization of vegetative stages, in order to compute the high initial growth rates measured in laboratory experiments of light deprivation when phytoplankton is brought back to sufficient irradiance levels after a dark period of several months (Peters and Thomas, 1996). The choice of the same respiration rate for diatoms and flagellates was necessary to obtain a dominance of diatoms but also a sufficient abundance of nanoflagellates, as observed in the station B area (Saggiomo et al., 2002).

Other important parameters are the availability coefficients of phytoplankton to grazers. Both grazing and iron are factors limiting the diatom bloom in the model. If iron limitation is deactivated in the model, the bloom is much larger and the time duration is totally controlled by grazing. The sensitivity of the model to grazing coefficients is rather high, particularly because the overwintering biomass is small and an excessive grazing pressure can completely deplete one of the phytoplankton group. This is for example the case of the simulated eukaryotic picophytoplankton, which is overgrazed by heterotrophic nanoflagellates living on bacteria. Nevertheless, it is difficult to assess the ecological relevance of this component (Vanucci and Bruni, 1998) and therefore we assumed that the microbial loop is limited to bacteria and their grazers. Bacterial biomass in the model is indeed strongly related to the predation pressure by heterotrophic nanoflagellates (HNAN). Synoptic measurements of bacterial activity and HNAN biomass (e.g. Vanucci and Bruni, 1999) are thus needed to achieve a larger confidence in the microbial activity rates produced by the model in the mesopelagic layer.

The physical evolution of the water column simulated by the model and shown in Sec. 3.1 is sufficient to provide the major physical mechanisms typical of this region. However, marginal ice zones are affected by a large degree of spatial variability and local physical conditions can be very different depending on the sea-ice distribution. We cannot expect the model to reproduce this variability, and particularly the Austral spring conditions where biogeochemical samples are collected in leads or in the wakes of the research vessels (Saggiomo et al., 1998). This implies that a lag of 1 or even 2 months in the evolution of the simulated phytoplankton bloom is likely to be ascribed to the forcing functions which are derived from low resolution datasets.

Although the timing of the bloom is difficult to be captured by the model, the esti-

mate of gross primary production and autotrophic chl-based biomass are in reasonable agreement with the available observations (Sec. 3.2). Phosphorus and nitrate drawdown are also within the observed ranges. The comparison with bottom traps, however, reveals some deficiencies in the simulation of organic matter utilization in the mesopelagic layer. Simulated microbial carbon consumption rates match the data (cfr. Sec. 3.4) but probably the nutrient utilization rates need to be further verified. The organic N flux at the bottom trap is in fact overestimated by the model, leading to a C:N ratio wich is about half the observed. The C:N ratios in simulated sinking detritus is a function of the actual ratio in the functional group that produces it. Since phytoplankton is allowed to uptake nutrients up to half the optimal ratio (set to Redfield, **?**), in nutrient-replete conditions the particulate derived from phytoplankton will have the same ratio unless nutrients are stripped from the organic matter by heterotrophic degradation. Modeled bacteria extract nutrients from the organic matter according to their requirements (Goldman et al., 1987), which are closer to the ratios found in the organic matter produced by nutrient-replete phytoplankton. It is therefore important to further verify the model parameterization of N uptake, comparing it with the available information on isotopic N upptake experiments (e.g. Lipizer et al., 2000; Cochlan and Bronk, 2001).

Silicate consumption in the surface layer is clearly underestimated with respect to the availabe data (Fig. 5). This is also confirmed by the underestimation of the BSi fluxes at the bottom trap (Fig. 9c). It is known that diatoms requires larger amount of silica in iron-depleted conditions (Takeda, 1998), but apparently even a 3 times higher Si:C ratio is not sufficient to reproduce the observations. In a model of the Kerguelen region, Pondaven et al. (2000) had to artificially increase this ratio up to 5 times to reproduce the observed silicate concentrations. The specific dissolution rate of BSi used in the model is already in the lower range of the measured rates

in the Southern ocean (Treguer et al., 1989, 0.01 d^{-1}), therefore the cause of this discrepancy is likely to be ascribed to the silica storage in diatom frustiles and the relationships with iron utilization and sinking rates which are still largely unknown.

Carbon production rates of diatoms are indeed in the range of the observed values as shown in Fig. 7. Model results also indirectly demonstrate how the physics may affect the physiological rate of phytoplankton and how different can be the estimates derived from standing stock measurements. The realized chl:C ratios are in fact always less varying than the theoretical value predicted by the Geider et al. (1996) parameterization, implying that the light-acclimation and the response to light of the average mixed layer population is different from the one derived from simpler parameterizations of light-limited growth. Models such as the BFM that takes into account these acclimation processes are therefore needed to appropriately capture this behavior.

The sensitivity analyses on detritus parameterization presented in Sec. 3.6 suggest that by varying the dimension and quality of the detrital particles we can obtain several patterns of vertical fluxes which have been actually observed in the Ross Sea sediment traps (DiTullio et al., 2000; Langone et al., 2000; Collier et al., 2000; Gardner et al., 2000; Langone et al., 2003; Asper and Smith, 2003). The succession of different phytoplankton groups is an important factor that contributes to the size-distribution and quality of organic detritus formed in the euphotic layer. The diatom dominance and the presence of nanoflagellates at station B lead to the concurrent production of larger and smaller particles that are likely to be the casue of the different deposition rates observed in the top and bottom traps. It can be hypothesized that the organic matter collected in the surface trap is directly related to the surface production, which is by nature subjected to the highly variable atmospheric and sea-ice conditions. The bottom trap on the other hand collects both freshly-produced

fast-sinking particles but also degraded slow-sinking material derived from the previous seasonal production phase. This detritus is accumulated throughout the year in the mesopelagic layer and the deposition flux is also probably modulated by three-dimensional advective processes, topographic features (Langone et al., 2000) and particle aggregation (Asper and Smith, 2003).

The timing of the bloom and of the deposition maxima are a major discrepancy in the comparison between trap data and simulation results. Apparently, the bloom at station B starts very early, already under packed ice conditions (Saggiomo et al., 1998) and the model cannot reproduce this feature. In addition, the fluxes in the top sediment trap suggest that there is a rapid decay of the bloom, which was not possible to simulate in the model with the current parameterization of grazers. We might also hipothesize that the bloom does not progress beyond January because of the presence of efficient predators which are not resolved in the model. Saggiomo et al. (1998) have reported the presence of krill attached to the ice fragments during the 1994 spring cruise which might exert a substantial control on the development of larger phytoplankton.

5 Final remarks

The Southern Ocean, and particularly the ocean regions around Antarctica are characterized by prolonged summer phytoplankton blooms that are visible in ocean color satellite images. The implications for the global ocean carbon cycle are substantial but the description of biogeochemical processes in these regions is still rather sketchy.

This work is a first approach to link the various kind of data collected during the Italian expeditions in the Ross Sea in order to provide an overview of the

mechanisms regulating the export of organic material to the ocean floor. The one-dimensional implementation obviously neglects the contributions of advective fluxes. However, this approach allowed to separate the contribution of local biogechemical processes and to identify how much of the observed variability can be explained by vertical dynamics only. The model can explain some of the patterns observed in the sediment traps, connecting it to production and consumption rates of the organic matter that have been compared with the available measurements. However, it is still to be demonstrated whether the model predictions on export rates can be extrapolated to the whole Ross Sea, and particularly to the polinya regions dominated by the colonial *Phaeocystis Antarctica*.

The results obtained from the modelling experiments, suggest a more comprehensive collection of biogeochemical rate measurements to be associated with the sediment trap timeseries. In particular the nature and composition of the sinking organic matter should be accurately estimated in order to improve the implemented parameterisations. This can lead to a more effective use of the modelling tool to better understand the processes involved in the Ross Sea carbon export dynamics.

Acknowledgements

This research was supported by the Italian projects BIOSESO I and II, funded by the Progetto Nazionale di Ricerca in Antartide initiative. MV was partly funded by the Italian project VECTOR for the adaptation of the BFM to the Ross Sea. P. Ruardij (NIOZ) is acknowledged for the availability of the OpenSesame simulation package.

References

Asper, V. L., Smith, W. O., 2003. Abundance, distribution and sinking rates of aggregates in the Ross Sea, antarctica. Deep-Sea Res. Pt. II 50, 131–150.

Azzaro, M., ferla, R. L., Azzaro, F., 2006. Microbial respiration in the aphotic zone of the Ross Sea (antarctica). Mar. Chem. 99, 199–209.

Baretta, J., Ebenhöh, W., Ruardij, P., 1995. The European Regional Seas Ecosystem Model, a complex marine ecosystem model. J. Sea Res. 33 (3-4), 233–246.

Baretta-Bekker, J., Baretta, J., Ebenhoeh, W., 1997. Microbial dynamics in the marine ecosystem model ERSEM II with decoupled carbon assimilation and nutrient uptake. J. Sea Res. 38 (3/4), 195–212.

Blumberg, A., Mellor, G., 1987. A description of a three-dimensional coastal ocean circulation model. In: Heaps, N. (Ed.), Three-dimensional coastal ocean model. American Geophysical Union, pp. 1–16.

Buesseler, K. O., 1991. Do upper-ocean sediment traps provide an accurate record of particle-flux? Nature 353, 420–423.

Buesseler, K. O., 1998. The decoupling of production and particulate export in the surface ocean. Glob. Biogeochem. Cy. 12, 297–310.

Cochlan, W. P., Bronk, D. A., 2001. Nitrogen uptake kinetics in the Ross Sea, Antarctica. Deep Sea Research II 48, 4127:4153.

Collier, R., Dymond, J., Honjo, S., Manganini, S., Francois, R., Dunbar, R., 2000. The vertical flux of biogenic and lithogenic material in the Ross Sea: moored sediment trap observations 1996-1998. Deep Sea Research II 47, 3491:3520.

Conkright, M., Garcia, H., O'Brien, T., Locarnini, R., Boyer, T., Stephens, C., Antonov, J., 2002. World Ocean Atlas 2001, Volume 4: Nutrients. Vol. NOAA Atlas NESDIS 52. U.S. Government Printing Office, Washington D.C., cD-ROMs.

URL http://www.nodc.noaa.gov/OC5/WOA01/woa01v4d.pdf

DiTullio, G. R., Grebmeier, J. M., Arrigo, K. R., Lizotte, M. P., Robinson, D. H., Leventer, A., Barry, J. P., VanWoert, M. L., Dunbar, R. B., 2000. Rapid and early export of Phaeocystis antarctica blooms in the Ross Sea, Antractica. Nature 404, 595:598.

DiTullio, G. R., Smith, W. O., 1996. Spatial patterns in phytoplankton biomass and pigment distributions in the Ross sea. Journal of Geophysical Research 101, 18467–18477.

Gardner, W. D., Richardson, M. J., Smith, W. O., 2000. Seasonal patterns of water column particulate organic carbon and fluxes in the Ross Sea, Antarctica. Deep Sea Research II 47, 3423:3449.

Geider, R., MacIntyre, H., Kana, T., 1996. A dynamic model of photoadaptation in phytoplankton. Limnol. Oceanogr. 41 (1), 1–15.

Goldman, J., Caron, D., Dennet, M., 1987. Regulation of gross growth efficiency and ammonium regeneration in bacteria by substrate C:N ratio. Limnol. Oceanogr. 32 (6), 1239–1252.

Goldman, J. C., Carpenter, E. J., 1974. A kinetic approach to the. effect of temperature on algal growth. Limnology and Oceanography 19.

Kwok, R., Comiso, J. C., 2002. Southern Ocean climate and sea ice anomalies associated with the Southern oscillation 15, 487–501.

Lancelot, C., Hannon, E., Becquevort, S., Veth, C., De Baar, H., 2000. Modeling phytoplankton blooms and carbon export production in the Southern Ocean: dominant controls by light and iron in the Atlantic sector in Austral spring 1992. Deep-Sea Res. Pt. II 47 (9), 1621–1662.

Langone, L., Dunbar, R. B., Mucciarone, D. A., Ravaioli, M., Meloni, R., Nittrouerand, C. A., 2003. Rapid Sinking of Biogenic Material During the Late Austral Summer in the Ross Sea, Antarctica. Vol. 78 of Antarctic Research Se-

ries Monograph. American Geophysical Union, pp. 221–234.

Langone, L., Frignani, M., Ravaioli, M., Bianchi, C., 2000. Particle fluxes and biogeochemical processes in an area influenced by seasonal retreat of the ice margin (northwestern Ross Sea Atarctica). Journal of Marine Systems 27, 221–234.

Ledley, T. S., Huang, Z., 1997. A possible ENSO signal in the Ross sea. Geophys. Res. Lett. 24, 3253–3256.

Lipizer, M., Mangoni, O., Catalano, G., Saggiomo, V., 2000. Phytoplankton uptake of ^{15}N and ^{14}C in the Ross Sea during austral spring 1994. Polar Biology 23, 495:502.

Mellor, G., Yamada, T., 1982. Development of a Turbulence Closure Model for Geophysical Fluid Problems. Rev. Geophys. Space Phys. 20 (4), 851–875.

Peters, E., Thomas, D. N., 1996. Prolonged darkness and diatom mortality I: Marine Antarctic species. Journal of Experimental Marine Biology and Ecology 207, 25:41.

Pondaven, P., Ruiz-pino, D., Fravalo, C., Treguer, P., Jeandel, C., 2000. Interannual variability of Si and N cycles at the time-series station KERFIX between 1990 and 1995 - A 1-D modelling study. Deep-Sea Res. Pt. I 47, 223–257.

Reynolds, R., 1988. A real-time global sea surface temperature analysis. J. Climate 1, 75–86.

Russo, A., Gallarato, A., Testa, G., Corbo, C., Pariante, M., 1997. Physical data collected during ROSSMIZE cruise (Ross sea,. November-December 1994). In: Faranda, F., Guglielmo, L., Povero, P. (Eds.), ROSSMIZE (Ross Sea Marginal Ice Zone Ecology) data report 1993-1995, Part I. Nat. Prog. Ant. Res., pp. 25–110.

Saggiomo, V., Carrada, G. C., Mangoni, O., d'Alcalá, M. R., Russo, A., 1998. Spatial and temporal variability of size-fractioned biomass and primary production in the Ross Sea (Antarctica) during austral spring and summer. Journal of Marine

Systems 17, 115:127.

Saggiomo, V., Catalano, G., Mangoni, O., Budillon, G., Carrada, G. C., 2002. Primary production processes in ice-free waters of the Ross Sea (Antarctica) during the austral summer 1996. Deep Sea Research II 49, 1787:1801.

Simmons, A., 2001. Development of the ERA-40 data-assimilation system. In: Workshop on Re-analysis. ECMWF, ECMWF, Reading, UK, pp. 11–30.
URL http://www.ecmwf.int/publications/library/ecpublications/proceedings/ERA40-reanalysis_workshop/index.html

Smith, W. O., Asper, V. L., 2001. The influence of phytoplankton assemblage composition on biogeochemical characteristics and cycles in the southern Ross Sea, Antarctica. Deep Sea Research I 48, 137:161.

Smith, W. O., Dunbar, R. B., 1998. The relationship between new production and vertical flux on the Ross Sea continental shelf. Journal of Marine Systems 17, 445–457.

Smith, W. O., Marra, J., Hiscock, M. R., Barber, R. T., 2000. The seasonal cycle of phytoplankton biomass and primary productivity in the Ross Sea, Antarctica. Deep Sea Research II 47, 3119:3140.

Smith, W. O., M.Nelson, D., Mathot, S., 1999. Phytoplankton growth rates in the Ross Sea, Antarctica, determined by independent methods: temporal variations. Journal of Plankton Research 21 (8), 1519:1536.

Smith, W. O., Nelson, D. M., DiTullio, G. R., Leventer, A. R., 1996. Temporal and spatial patterns in the Ross Sea: phytoplankton biomass, elemental composition, productivity and growth rates. Journal of Geophysical Research 101 (C8), 18455:18465.

Sosik, H. M., Olson, R. J., 2002. Phytoplankton and iron limitation of photosynthetic efficiency in the Southern Ocean during late summer. Deep Sea Research

I 49, 1195:1216.

Takeda, S., 1998. Influence of iron availability on nutrient consumption ratio of diatoms in oceanic waters. Nature 393, 774–777.

Treguer, P., Kamatani, A., Gueneley, S., Queguiner, B., 1989. Kinetics of dissolution of antarctic diatom frustules and the biogeochemical cycle of silicon in the Southern Ocean. Polar Biology 9, 397–403.

Uppala, S., 2001. ECMWF Re-Analysis 1957-2001, ERA-40. In: Workshop on Re-analysis. ECMWF, ECMWF, Reading, UK, pp. 11–30.
URL http://www.ecmwf.int/publications/library/ecpublications/proceedings/ERA40-reanalysis_workshop/index.html

Vaillancourt, R. D., Marra, J., Barber, R. T., Smith, W. O., 2003. Primary productivity and in situ quantum yields in the Ross Sea and Pacific Sector of the Antarctic Circumpolar Current. Deep Sea Research II 50, 559:578.

Vanucci, S., Bruni, V., 1998. Presence or absence of picophytoplankton in the western ross sea during spring 1994: a matter of size definition? Polar Biology 20, 9:13.

Vanucci, S., Bruni, V., 1999. Small nanoplankton and bacteria in the Western Ross Sea during sea-ice retreat (spring 1994). Polar Biology 22, 311:321.

Vichi, M., Ruardij, P., Baretta, J. W., 2004. Link or sink: a modelling interpretation of the open Baltic biogeochemistry. Biogeosciences 1, 79–100.

	D0	D1	D2	D3	D4	D5
Number of DET variables	1	2	2	2	2	2
$R^{(5)}$ sinking rate (m d^{-1})	-	10	10	10	100	100
$R^{(6)}$ sinking rate (m d^{-1})	1.5	1.5	1.5	1.5	1.5	1.5
$R^{(5)}$ degradation rate (d^{-1})	-	0.1	0.01	0.5	0.01	0.5
$R^{(6)}$ degradation rate (d^{-1})	0.01	0.01	0.01	0.01	0.01	0.01

Table 1

List of sensitivity experiments on the detritus sinking and degradation rates. $R^{(5)}$and $R^{(6)}$ are the fast- and slow-sinking components of detritus, respectively (cfr. Fig. 2). D5 is the reference simulation shown in Sec. 3.

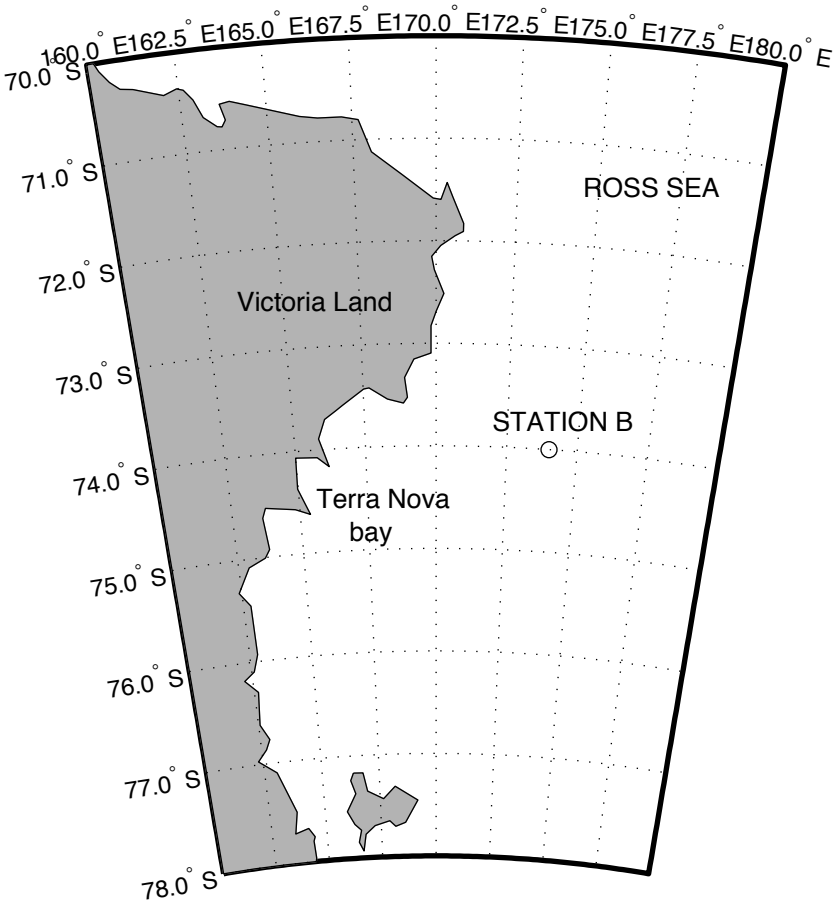

Figure 1. Map showing the location of station B in the Ross Sea.

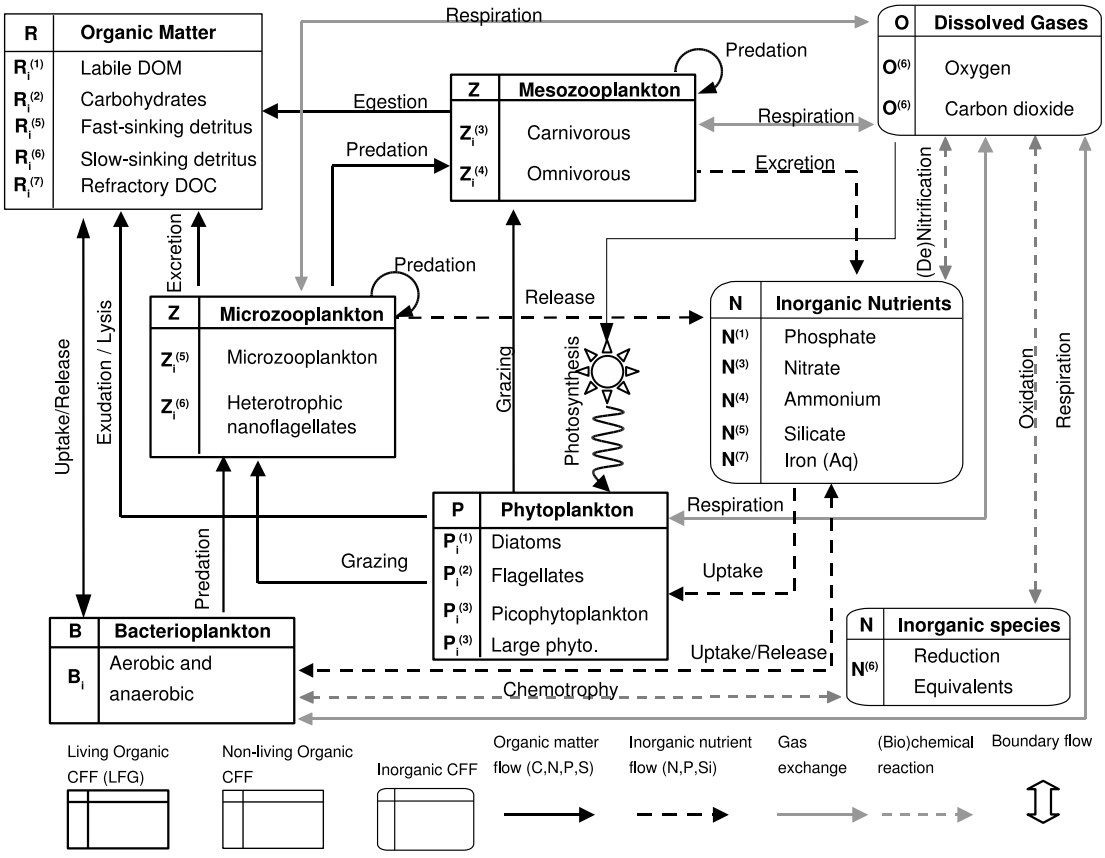

Figure 2. Scheme of the pelagic BFM model with state variables divided in living, non-living and inorganic Chemical Functional Families. The arrows represent the exchanges of inorganic and organic matter according to the major physiological and ecological processes.

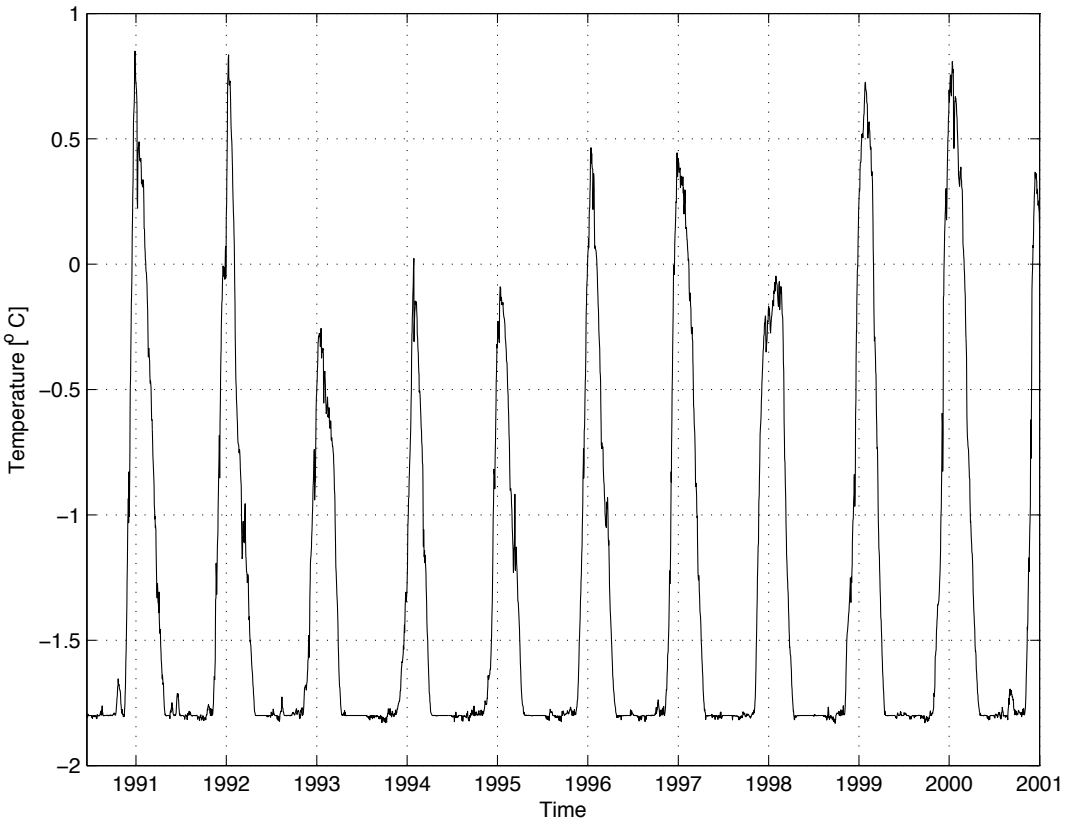

Figure 3. Timeseries of simulated sea surface temperature at station B.

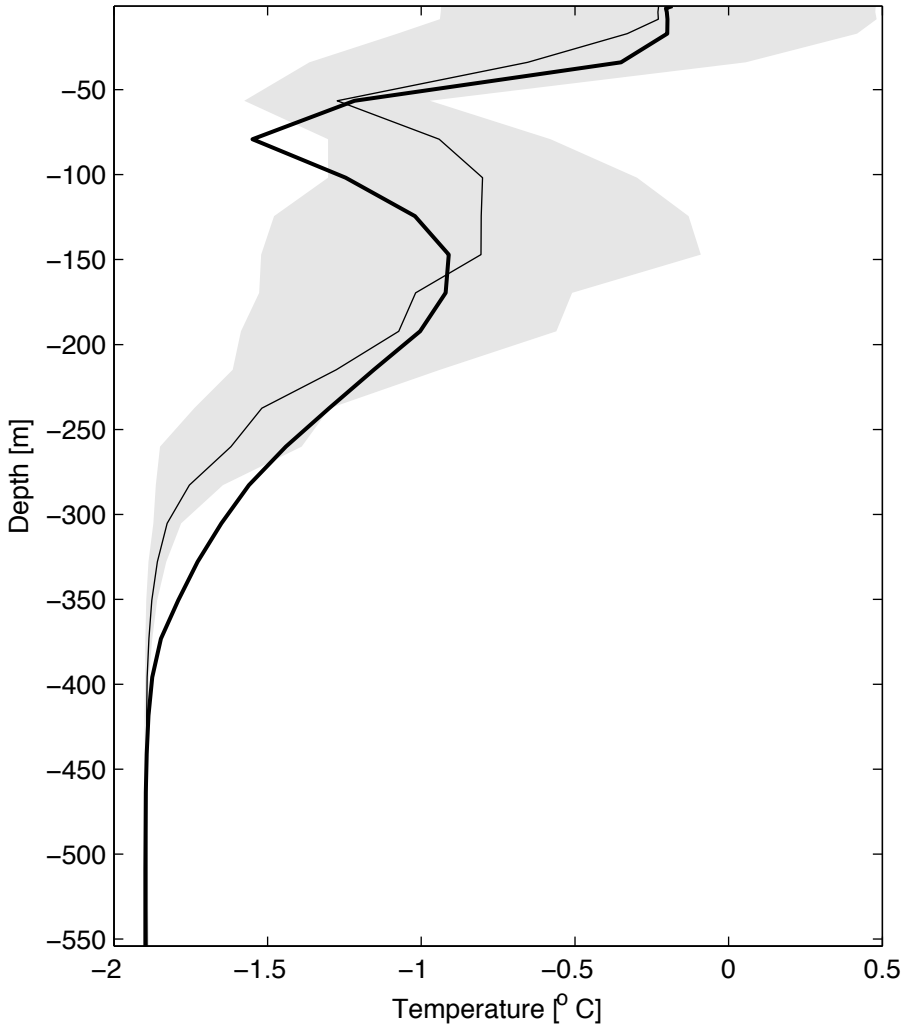

Figure 4. Simulated (thick line) and observed (dashed line plus standard deviation in gray shading) temperature profile at station B over the period 1995-1998. Data have been interpolated to the model levels.

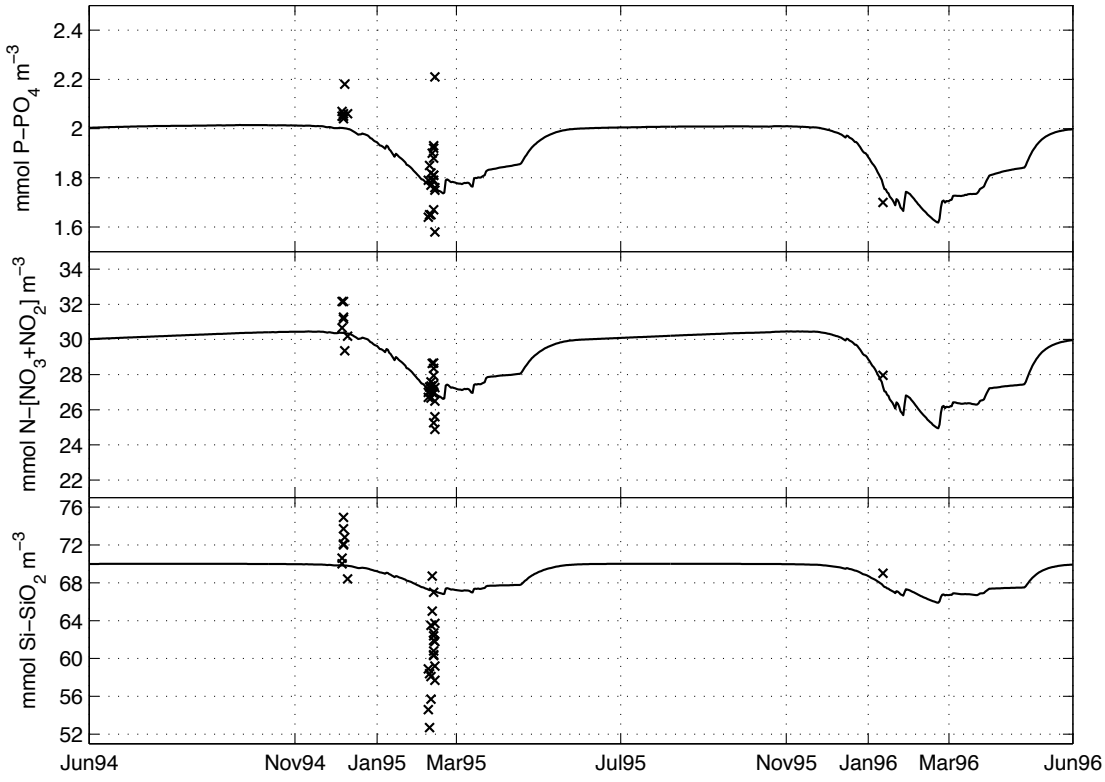

Figure 5. Simulated (continuous line) and observed (crosses) concentrations of dissolved macronutrients at station B: (a) phosphate, (b) nitrate + nitrite, (c) silicate.

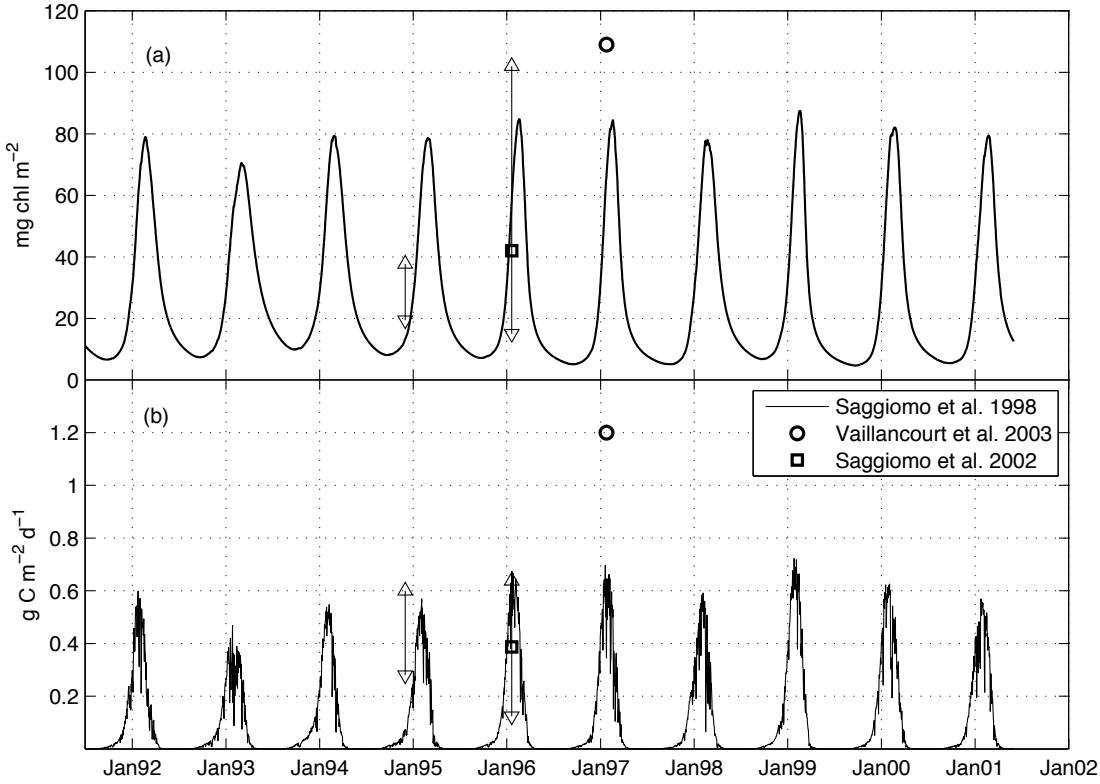

Figure 6. (a) Simulated phytoplankton chlorophyll and (b) gross primary production integrated over the first 100 m. Data and ranges of variability from Saggiomo et al. (1998, 2002); Vaillancourt et al. (2003) are indicated as reference for the station B area.

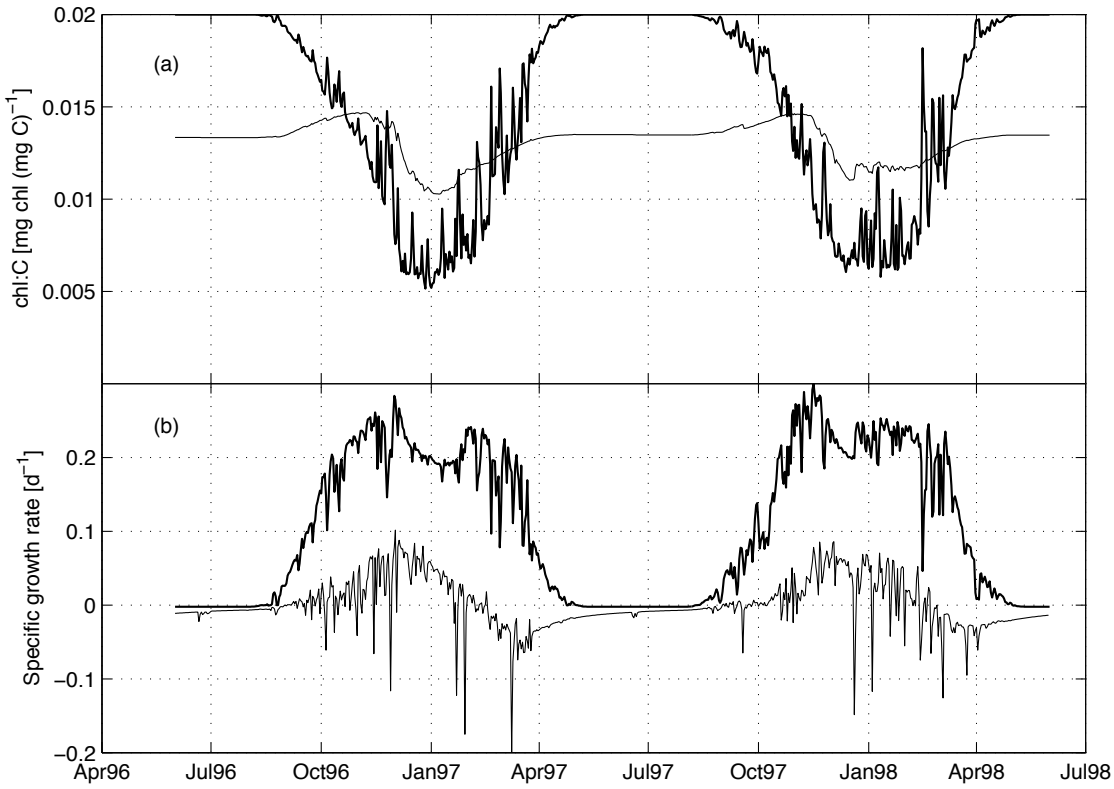

Figure 7. (a) Simulated chl:C ratio in surface diatoms. Thick line: potential theoretical ratio; thin line: realized ratio. (b) Simulated specific growth rate of surface diatoms. Thick line: computed as photosynthesis - respiration - excretion; thin line: estimated from carbon biomass concentration.

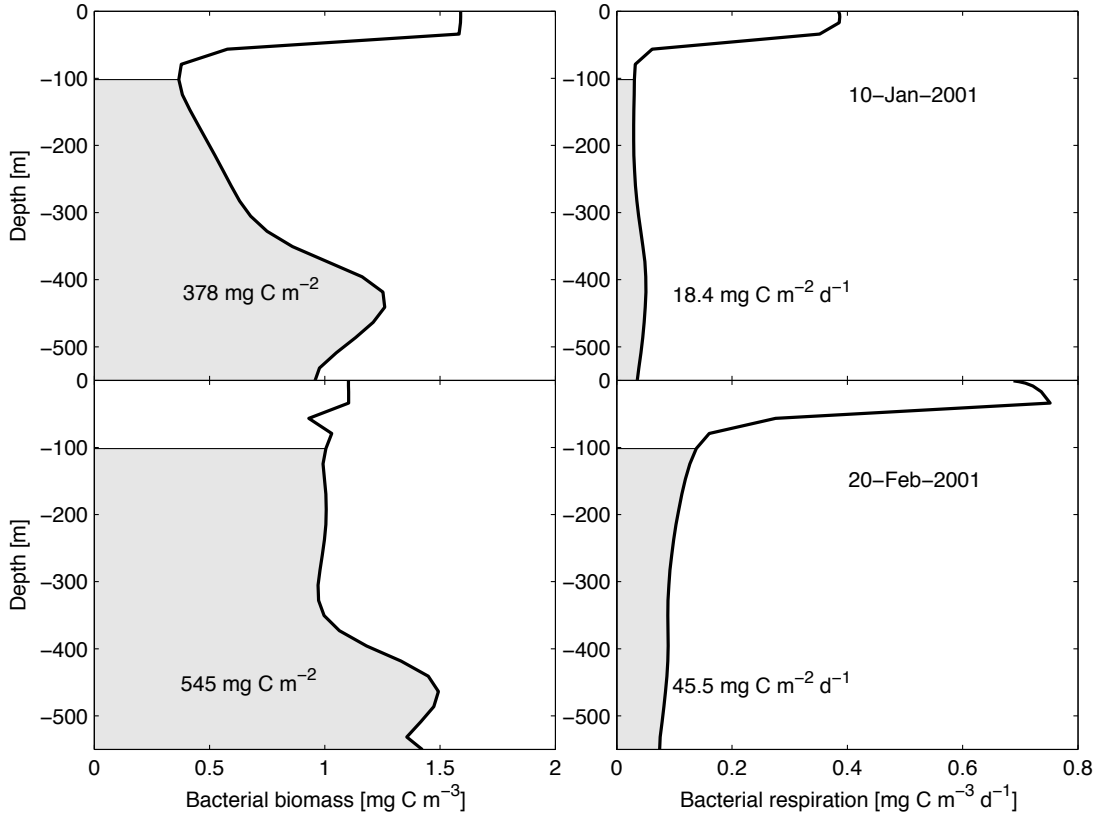

Figure 8. Simulated profiles of bacterial biomass and respiration rates on January 10, 2001 (top panels) and February 20, 2001 (bottom panels). Integrated values in the mesopelagic layer (shaded area) are also given for comparison with observations (Azzaro et al., 2006).

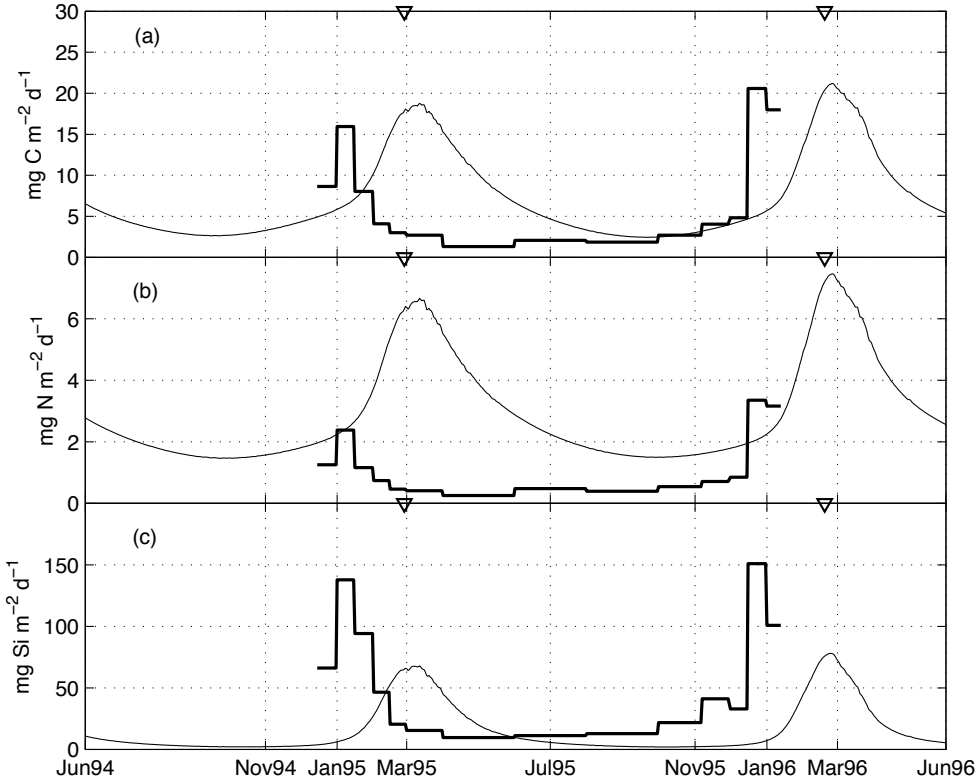

Figure 9. Observed (thick line) and simulated organic matter fluxes at the bottom sediment trap (550 m) for (a) organic C, (b) organic N and (b) biogenic Si. The triangles mark the occurrences of the surface biomass peaks in 1995 and 1996.

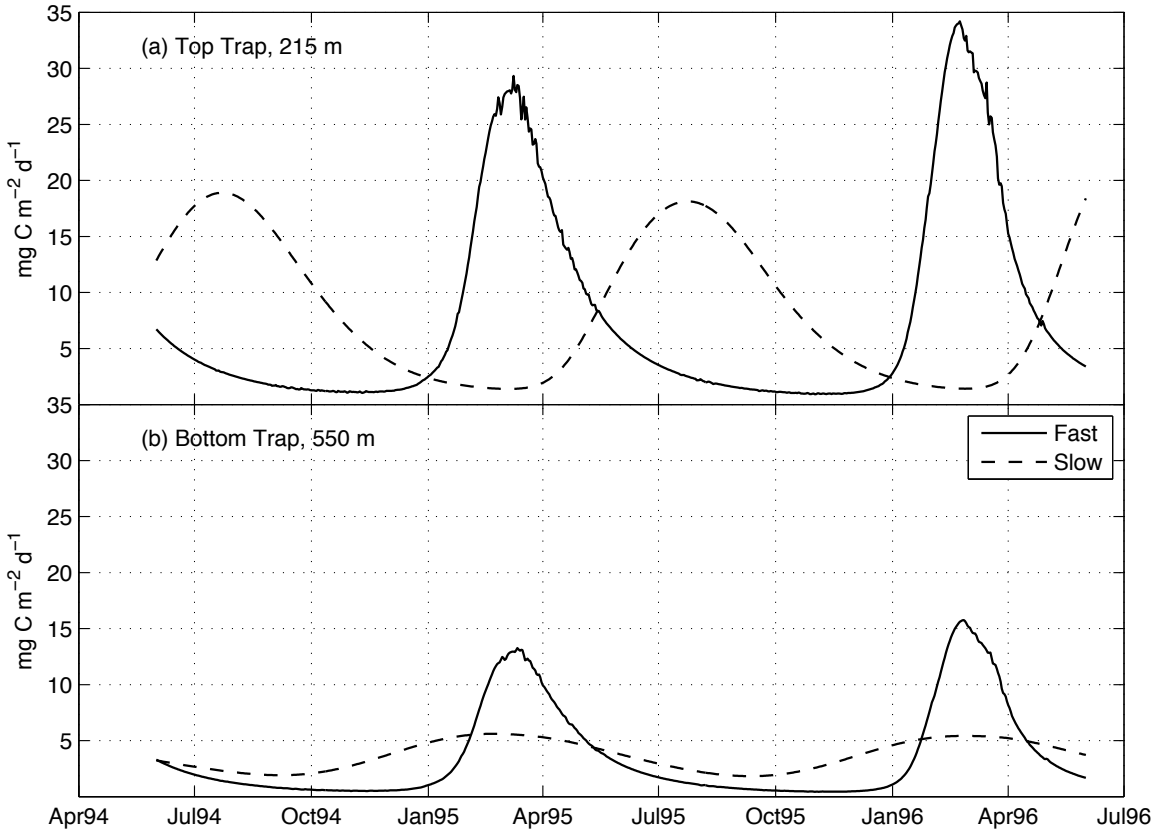

Figure 10. Contribution of the two types of detritus to the simulated organic carbon fluxes in the (a) top and (b) bottom sediment traps.

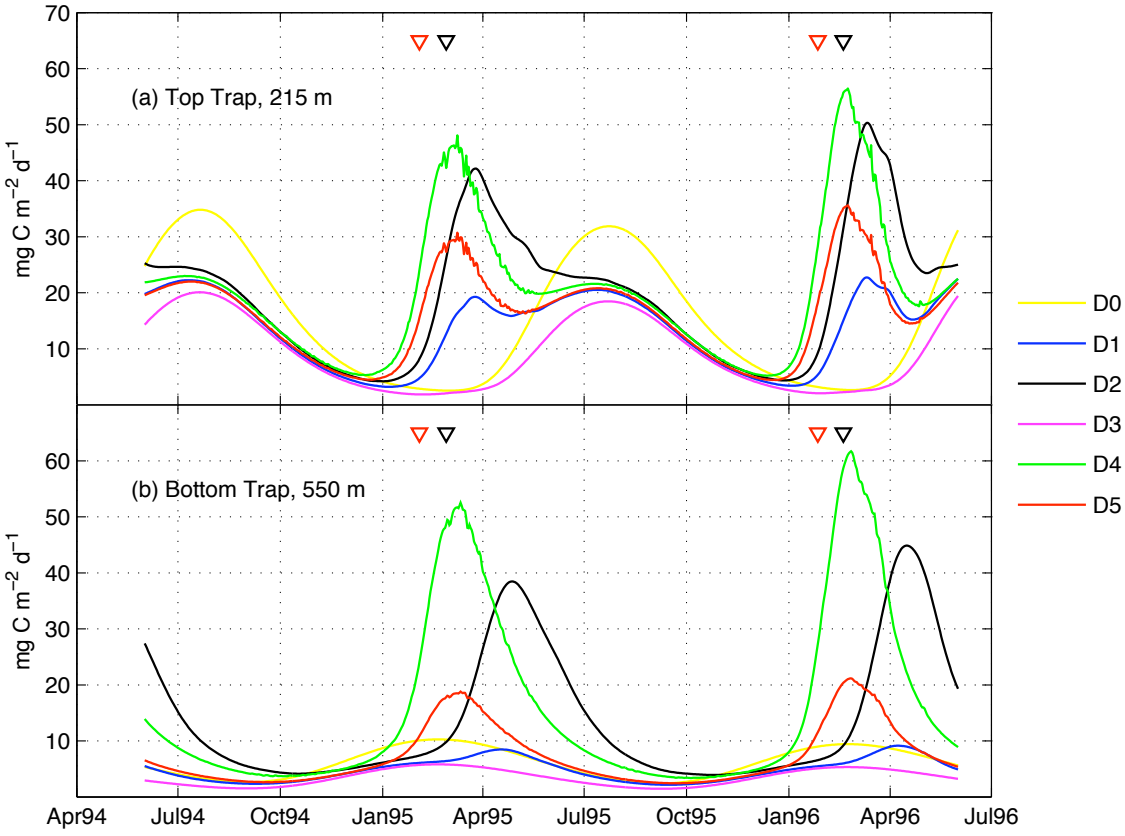

Figure 11. Sensitivity analysis on the simulated fluxes at the sediment traps (a) top and (b) bottom. The red and blue triangles mark the peaks of surface production and biomass for each year, respectively. Experiment details are given in Table 1.